

Sampled Nonlocal Gradients for Stronger Adversarial Attacks

Leo Schwinn¹, Daniel Tenbrinck², An Nguyen¹, René Raab¹, Martin Burger², Bjoern Eskofier¹

¹ Machine Learning and Data Analytics Lab (MaD Lab), Department of Computer Science

² Department of Mathematics

Friedrich-Alexander University Erlangen-Nürnberg, Germany

Abstract

The vulnerability of deep neural networks to small and even imperceptible perturbations has become a central topic in deep learning research. The evaluation of new defense mechanisms for these so-called adversarial attacks has proven to be challenging. Although several sophisticated defense mechanisms were introduced, most of them were later shown to be ineffective. However, a reliable evaluation of model robustness is mandatory for deployment in safety-critical real-world scenarios. We propose a simple yet effective modification to the gradient calculation of state-of-the-art first-order adversarial attacks, which increases their success rate and thus leads to more accurate robustness estimates. Normally, the gradient update of an attack is directly calculated for the given data point. In general, this approach is sensitive to noise and small local optima of the loss function. Inspired by gradient sampling techniques from non-convex optimization, we propose to calculate the gradient direction of the adversarial attack as the weighted average over multiple points in the local vicinity. We empirically show that by incorporating this additional gradient information, we are able to give a more accurate estimation of the global descent direction on noisy and non-convex loss surfaces. Additionally, we show that the proposed method achieves higher success rates than a variety of state-of-the-art attacks on the benchmark datasets MNIST, Fashion-MNIST, and CIFAR10.

Introduction

Deep learning has led to breakthroughs in various fields, such as computer vision (Krizhevsky, Sutskever, and Hinton 2012; He et al. 2016) and language processing (van den Oord et al. 2016). Despite its success, it is still limited by its vulnerability to adversarial examples (Szegedy et al. 2014). In image processing, adversarial examples are small, typically imperceptible perturbations to the input that can lead to misclassifications in real-world scenarios. In domains like autonomous driving or healthcare this can potentially have fatal consequences. Since the weakness of neural networks to adversarial examples has been demonstrated, many methods were proposed to make neural networks more robust and reliable (Goodfellow, Shlens, and Szegedy 2015; Madry et al. 2018; Tramèr and Boneh 2019). In a constant challenge between new adversarial attacks and defenses, most of the proposed defenses have been shown to be rather ineffective (Guo et al. 2018; Kurakin et al. 2018; Samangouei, Kabkab,

and Chellappa 2018). Yet, substantial progress in this field is needed to increase the reliability and trustworthiness of neural networks in our daily lives.

In this paper we aim to improve the effectiveness of adversarial attacks on artificial neural networks. For this we adopt an intuitive idea that is known as gradient sampling (Burke, Lewis, and Overton 2005). This method is designed to reliably estimate the significant optima of non-smooth non-convex functions with unreliable gradient information. Gradient sampling can be interpreted as a generalized steepest descent method where the gradient is not only calculated at a given point but additionally for points in the direct vicinity. The final gradient direction is subsequently calculated in the convex hull of all sampled gradients and thus incorporates additional information about the local geometry of the loss surface. The central idea behind this approach is that point estimates of gradients can be misleading, especially for noisy and non-convex loss surface. However, this method is only feasible for low-dimensional functions, due to the complexity of computing the convex hull in higher dimensions. To overcome this problem, we propose to simplify the algorithm so that it works with high dimensional data. We discard the calculation of the convex hull and compute the final gradient direction as a weighted average of all sampled gradients. Figure 1 illustrates how the convergence of the standard Gradient Descent (GD) method can be improved for noisy and non-convex loss surfaces by the proposed Sampled Nonlocal Gradient Descent (SNGD). Standard GD calculates nearly random ascent directions while SNGD approximates the global ascent direction more accurately as it is less susceptible to noise and local optima.

The contributions of this paper can be summarized as follows. First we relate the proposed gradient sampling method to the empirical mean, which converges towards a nonlocal gradient with respect to an underlying probability distribution for enough sampling operations. Subsequently we show that SNGD-based attacks are more query efficient while achieving higher success rates than prior attacks on popular benchmark datasets. Finally, we demonstrate that SNGD approximates the direction of an adversarial example more accurately during the attack and empirically show the effectiveness of SNGD on non-convex loss surfaces.

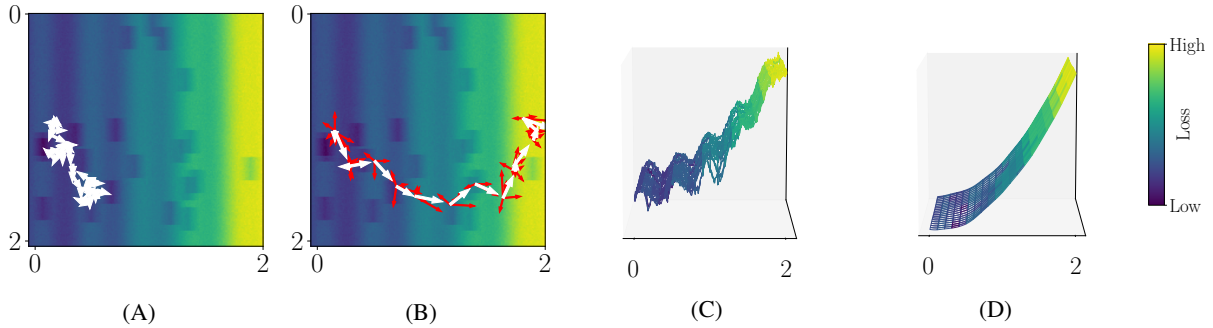


Figure 1: Comparison between the standard Gradient Descent (GD) method (A) and the proposed Sampled Nonlocal Gradient Descent (SNGD) (B). (C) shows the side view of the noisy loss surface displayed in (A) and (B). The calculated ascent direction is displayed by a white arrow. For SNGD the ascent direction is obtained by averaging multiple gradients (red arrows) in the vicinity of the current point on the loss surface. (D) illustrates the effect of SNGD when the amount of sampling operations N tends to infinity. In the limit, using SNGD is equivalent to using GD on a loss surface that is convoluted with a convolution kernel defined by the sampling distribution.

Preliminary

In the following we introduce the necessary mathematical notation to describe adversarial attacks and to review current contributions in this field.

Notation

Let (x, y) with $x \in \mathbb{R}^d$ and $y \in \{1, 2, \dots, C\}$ be pairs of samples and labels in a classification task with C different classes, where each sample is represented by a d -dimensional feature vector. In the following we assume that the samples are drawn from the d -dimensional unit cube, i.e., $x \in [0, 1]^d$, as this is typically the case for image data. Let \mathcal{L} be the loss function (e.g., categorical cross-entropy) of a neural network F_θ , parameterized by the parameter vector $\theta \in \Theta$. Constructing an adversarial perturbation $\gamma \in \mathbb{R}^d$ with maximum effect on the loss value can be stated as the following optimization problem:

$$\max_{\gamma} \mathcal{L}(F_\theta(x + \gamma), y) \quad (1)$$

The perturbation γ is usually constrained in two ways: 1) The value range of the adversarial example is still valid for the respective domain (e.g, between $[0, 1]$ or $[0, 255]$ for images), 2) The adversarial example $x_{adv} = x + \gamma$ is within a set of allowed perturbations S that are unlikely to change the class label for human perception. In the following, we focus on *untargeted gradient-based adversarial attacks* that are constrained by the L_∞ norm such that $\|\gamma\|_\infty \leq \epsilon$, as done in prior work (Lin et al. 2020).

Related Work

A variety of adversarial attacks have been proposed. We give a brief overview for the most successful gradient-based algorithms and also a proven zeroth order attack known as Simultaneous Perturbation Stochastic Approximation (SPSA).

Fast Gradient Sign Method (FGSM) FGSM introduced by Goodfellow, Shlens, and Szegedy, is one of the first

gradient-based adversarial attacks. FGSM calculates an adversarial example according to the following equation:

$$x_{adv} = \Pi_S(x + \epsilon \cdot \text{sign}(\nabla_x \mathcal{L}(F_\theta(x), y))) \quad (2)$$

where $\Pi_S(x)$ is a projection operator that keeps γ within the set of valid perturbations S and sign is the componentwise signum operator.

Basic Iterative Method (BIM) Kurakin, Goodfellow, and Bengio proposed an iterative variant of the FGSM attack, in which multiple smaller gradient updates are used to find the adversarial perturbation:

$$x_{adv}^{t+1} = \Pi_S(x_{adv}^t + \alpha \cdot \text{sign}(\nabla_x \mathcal{L}(F_\theta(x_{adv}^t), y))) \quad (3)$$

where $\epsilon \geq \alpha > 0$ and x_{adv}^{t+1} describes the adversarial example at iteration t and $x_{adv}^0 = x$. Madry et al. introduced a slightly modified version of BIM called **Projected Gradient Descent (PGD)**, in which the starting point of the attack is randomly chosen from the set of valid perturbations S . More variants of iterative gradient-based attacks have been proposed. This includes several momentum-based methods (Dong et al. 2018; Uesato et al. 2018; Lin et al. 2020) MI-FGSM ADAM-PGD, NI-FGSM.

Nesterov Iterative Fast Gradient Sign Method (NI-FGSM) Lin et al. incorporated Nesterov momentum into iterative attacks to improve their transferability and success rate. The attack is formally given by:

$$\begin{aligned} x_{nes}^t &= x_{adv}^t + \alpha \cdot \mu \cdot g^t \\ g^{t+1} &= \mu \cdot g^t + \frac{\nabla_x \mathcal{L}(F_\theta(x_{nes}^t), y)}{\|\nabla_x \mathcal{L}(F_\theta(x_{nes}^t), y)\|_1} \\ x_{adv}^{t+1} &= \Pi_S(x_{adv}^t + \alpha \cdot \text{sign}(g^{t+1})) \end{aligned} \quad (4)$$

where g^t denotes the accumulated gradients at iteration t and $g^0 = 0$ and $x_{adv}^0 = x$. $\mu > 0$ describes the momentum parameter.

Output Diversified Initialization (ODI) Tashiro, Song, and Ermon introduced ODI, which aims at finding efficient starting points for adversarial attacks. Therefore, they calculate the starting point of an adversarial attack such that it maximizes the difference in the output space compared to a clean sample. They empirically show that this initialization provides more diverse and effective starting points than random initialization. The initialization of an ODI-based attack is given by:

$$x_{ODI}^{t+1} = \Pi_S(x_{adv}^t + \alpha \cdot \text{sign}\left(\frac{\nabla_x \omega^\top F_\theta(x_{ODI}^t)}{\|\nabla_x \omega^\top F_\theta(x_{ODI}^t)\|_2}\right)) \quad (5)$$

where $x_{adv}^0 = x$ and $\omega \in \mathbb{R}^C$ is sampled from a uniform distribution in a predefined range. This procedure is repeated for a given number of steps. Afterwards, the calculated starting point can be used for initializing an adversarial attack.

Brendel & Bethge Attack (B&B) Brendel et al. propose an alternative gradient-based attack. They use gradients to estimate the decision boundary between an adversarial and a benign sample. Subsequently the attack follows the decision boundary towards the clean input to find the smallest perturbation that leads to a misclassification. Simultaneously, the updated perturbation is forced to stay within a box-constraint of valid inputs. The optimization problem can be formulated as follows:

$$\begin{aligned} \min_{\delta} \quad & \|x - x_{adv}^{t-1} - \delta^t\|_\infty \quad \text{s.t.} \\ & x - x_{adv}^{t-1} + \delta^t \in [0, 1]^d, \quad b^{\top} \delta^t = c^t, \quad \|\delta^t\|_2^2 \leq r \end{aligned} \quad (6)$$

where $\delta^t \in \mathbb{R}^d$ is the step along the decision boundary in iteration $t \in \mathbb{N}$ within a given trust region with radius $r > 0$, b^t denotes the current estimate of the normal vector of the local boundary, and c^t describes the constraint that the current perturbation is on the decision boundary. In particular the L_∞ -variant of this attack is of interest for our investigations.

Simultaneous Perturbation Stochastic Approximation (SPSA) proposed by (Spall 1992; Uesato et al. 2018) is a zeroth order optimization algorithm which has been successfully used in prior work to break models with obfuscated gradients (Uesato et al. 2018). It uses finite-differences to approximate the optimal descent direction. Zeroth order attacks are usually less efficient than their gradient-based counterparts. Nevertheless, they can be used in situations where the gradient information of the model is either removed by a non-differentiable operation (e.g., JPEG compression (Guo et al. 2018)) or is highly obfuscated, as described in (Kurakin et al. 2018).

Sampled Nonlocal Gradient Descent

We propose an alternative to the standard Gradient Descent (GD) algorithm, which we name Sampled Nonlocal Gradient Descent (SNGD). Our aim is to use this method to further augment existing gradient-based attacks. SNGD is specifically designed for noisy and non-convex loss surfaces as it calculates the gradient direction as the weighted average over multiple sample points in the vicinity of the current

data point. The gradient calculation of SNGD is given by:

$$\begin{aligned} \nabla_{SNGD} \mathcal{L}(F_\theta(x, y)) &:= \\ \nabla_x \frac{1}{N} \sum_{i=1}^N w_i \cdot \mathcal{L}(F_\theta(\text{clip}_{[0,1]}\{x + \xi_i^\sigma\}, y)), \end{aligned} \quad (7)$$

where $N \in \mathbb{N}$ is the number of sampling operations, w_i is the i -th weight of a sampled gradient, and $\text{clip}_{[a,b]}$ is the component-wise clipping operator with value range $[a, b]$. The clipping operator is needed to ensure that the data stays in the normalized range, e.g., in the case of images. It can be discarded for other applications with unbounded data. The random variables ξ_i^σ are considered to be drawn i.i.d. from a distribution P^σ parametrized by the standard deviation $\sigma > 0$, which effectively determines the size of the neighborhood. By the law of large numbers the sampled nonlocal gradient converges (with a rate of order $N^{-1/2}$ in variance) to the respective expectation value, which is the given by the following nonlocal gradient

$$\nabla_x \mathbb{E}_{\xi \sim P^\sigma} [\mathcal{L}(F_\theta(\text{clip}_{[0,1]}\{x + \xi\}, y))] \quad (8)$$

The expectation is effectively a local averaging of the likelihood around x . Note that by linearity the proposed SNGD method is equivalent to an averaging of the gradients, i.e., the standard form of a nonlocal gradient, cf. (Du 2019). This observation is also useful to efficiently compute the attack, as one can use only a single backward pass for all sampled gradients in each iteration. Note that as the forward-passes can be parallelized, the effective runtime of SNGD is equivalent to GD with sufficient memory. A SNGD-based BIM attack is formally given by:

$$x_{adv}^{t+1} = \Pi_S(x_{adv}^t + \alpha \cdot \text{sign}(\nabla_{SNGD} \mathcal{L}(F_\theta(x_{adv}^t), y))) \quad (9)$$

We demonstrate the benefit of this approach in terms of efficiency in the results section below.

Experiments

We conduct several experiments to evaluate SNGD. We first analyze if SNGD can improve the success rate of adversarial attacks compared to GD. Secondly, we explore the possibility of combining SNGD with other methods, e.g., ODI. Also we investigate the option to decay the standard deviation σ during an attack and to individually weight the sampled gradients. Furthermore, we inspected the performance difference between several attacks, as efficient attacks play an important role to facilitate the evaluation of model robustness in real-world applications. Lastly, we analyze the ability of SNGD to better approximate the global descent direction and show that SNGD is effective for non-convex loss surfaces. Additional and ineffective experiments are included in the supplementary material.

Setup

In the following we give an overview of general hyperparameters used for the experiments, including thread model, training, evaluation, and datasets. We describe dataset-specific hyperparameters such as the model architecture in the corresponding sections.

Threat model In this work we focus our evaluation on the L_∞ norm and untargeted attacks. We combine our proposed method, SNGD with state-of-the-art attacks, including PGD (Madry et al. 2018) and PGD with Nesterov Momentum (N-PGD) (Lin et al. 2020), which we call SN-PGD and SN-N-PGD respectively. We additionally combine all PGD-based attacks with ODI (Tashiro, Song, and Ermon 2020). ODI-based attacks achieve one of the highest Success rates on the Madry MNIST leaderboard (Madry et al. 2018). Moreover, we compare our approach to the B&B attack (Brendel et al. 2019), one of the most recent and effective gradient-based attacks. We additionally evaluated if models are obfuscating their gradients with the zeroth order SPSA attack (Spall 1992; Uesato et al. 2018). If not stated otherwise all SNGD-based attacks are performed with $w_i = 1, \forall i \in \{1, 2, \dots, N\}$.

We limited the amount of model evaluations to 2000 for each gradient-based attack and distributed them over multiple restarts and samples (SNGD), such that $R \cdot I \cdot N = 2000$, where R denotes the total number of restarts, I the amount of attack iterations, and N the amount of sampling operations for SNGD. We tried multiple combinations of model evaluations and restarts, as we observed that for a fixed budget of total evaluations this considerably impacts the performance of the attacks. For the standard PGD attack we obtained the highest success rates between 20 – 400 iterations and 5 – 100 random restarts. For SN-PGD attacks we used 100 iterations, 4 sampling operations and 5 random restarts. The B&B attack was performed with 1000 iterations and two restarts. The SPSA attack was performed with 100 steps and a sample size of 8192, as shown to be effective in (Uesato et al. 2018). Additional hyperparameters are included in the supplementary material. We performed all attacks on the same subset of 1000 (10%) randomly selected test images as in (Uesato et al. 2018; Brendel et al. 2019).

Data and architectures

Three different image classification datasets were used to evaluate the adversarial robustness of the different models (MNIST (LeCun et al. 1998), Fashion-MNIST (Xiao, Rasul, and Vollgraf 2017) and CIFAR10 (Krizhevsky 2009)). We split each dataset into the predefined train and test sets and additionally removed 10% (5000 samples) of the training data for validation.

Training We decided to evaluate our attack on two of the strongest empirical defenses to date, adversarial training (Athalye, Carlini, and Wagner 2018; Madry et al. 2018; Uesato et al. 2018) and TRADES (Zhang et al. 2019). For adversarial training we used the fast FGSM-based adversarial training algorithm (Wong, Rice, and Kolter 2020). In preliminary experiments on MNIST we observed that the loss surfaces of these models are not as convex as described in prior work (Kurakin et al. 2018; Chan et al. 2020) (see Figure 4A) compared to models trained with PGD-based adversarial training. For comparison we additionally trained each model with the typically used PGD-based adversarial training (Madry et al. 2018). For TRADES we used the pre-trained model provided by the authors of the original paper

(Zhang et al. 2019) for the MNIST and CIFAR10 datasets.

For fast FGSM-based training we used the same hyperparameters as proposed in (Wong, Rice, and Kolter 2020). For PGD-based training we used 7 steps and a step size of $1/4 \epsilon$ (Madry et al. 2018). All self-trained networks were trained and evaluated 5 times using stochastic gradient descent with the Adam optimizer ($\beta_1 = 0.9, \beta_2 = 0.999$) (Kingma and Ba 2015). We used a cyclical learning rate schedule (Smith 2017) which has been successfully used for adversarial training in prior work (Wong, Rice, and Kolter 2020). Thereby, the learning rate λ is linearly increased up to its maximum Λ over the first $2/5$ epochs and then decreased to zero over the remaining epochs. The maximum learning rate Λ was estimated by increasing the learning rate of each individual network for a few epochs until the training loss diverged (Wong, Rice, and Kolter 2020). All models were optimized for 100 epochs, which was sufficient for convergence, and the checkpoint with the lowest adversarial validation loss was chosen for testing.

MNIST consists of greyscale images of handwritten digits each of size $28 \times 28 \times 1$ (60,000 training and 10,000 test). We used the same MNIST model that Wong, Rice, and Kolter used for fast adversarial training. However, we doubled the number of filters for the convolutional layers, as we noticed that the performance of the model sometimes diverged to random guessing during training. The optimal maximum learning rate we found for MNIST was about 0.005, which is in line with (Wong, Rice, and Kolter 2020). As in prior work, we used a maximum perturbation budget of $\epsilon = 0.3$.

Fashion-MNIST consists of greyscale images of 10 different types of clothing, each of size $28 \times 28 \times 1$ (60,000 training and 10,000 test). The Fashion-MNIST classification task is slightly more complicated than MNIST, as it contains more intricate patterns. For Fashion-MNIST we used the same architecture as for MNIST. The optimal learning rate we found for Fashion-MNIST was approximately 0.007. To the best of our knowledge there is no standard perturbation budget ϵ commonly used for Fashion-MNIST. Since this dataset contains more complicated patterns than MNIST we used a lower maximum perturbation budget of $\epsilon = 0.15$.

CIFAR10 consists of color images, each of size $32 \times 32 \times 3$, with 10 different labels (50,000 training and 10,000 test). CIFAR10 is the most challenging classification task out of the three. For CIFAR10 we used the same PreActivation-ResNet18 (He et al. 2016) architecture as in (Wong, Rice, and Kolter 2020). All images from the CIFAR10 dataset were standardized and random cropping and horizontal flipping were used for data augmentation during training as in (He et al. 2016; Madry et al. 2018; Wong, Rice, and Kolter 2020). We found the optimal learning rate to be around 0.21. Inline with previous work, we set the maximum perturbation budget to $\epsilon = 8/255$.

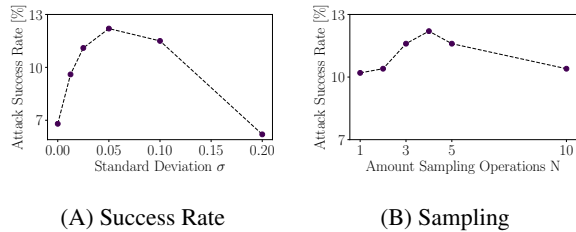


Figure 2: The two plots show the success rate of SNGD-based PGD attacks (SN-PGD) on a single validation batch (512 samples) of the **MNIST** dataset ($\epsilon = 0.3$). **(A)** SN-PGD success rate for varying standard deviations σ . All displayed attacks are performed with 100 iterations, 5 restarts and $N = 4$. For noise free attacks ($\sigma = 0$) we made an exception and used 400 iterations and 5 restarts. **(B)** SN-PGD success rate for different amounts of sampling operations N and $\sigma = 0.05$. Every attack was performed with 5 restarts and the amount of attack iterations I was set to $400/N$.

Experiments on noise distributions and sampling

Noise distribution: To combine SNGD with an adversarial attack we need to define the distribution P^σ from which we sample data points in the local neighborhood. In preliminary experiments we evaluated the performance for the Uniform, Gaussian and Laplacian distributions on the MNIST dataset. We analyzed the success rate for a wide range of distribution parameters but did not observe any considerable differences between the optimally tuned distributions. Since the Gaussian distribution achieved marginally superior results, we decided to use it for the remaining experiments.

We constrained the search space for the optimal standard deviation σ to $0 < \sigma < \epsilon$ since the gradient information outside of the attack radius should be non-relevant for the optimization of the attack. To rapidly find a good estimate for the standard deviation σ for each model and attack, we fine-tuned σ on a single batch of the validation set. We observed that for a wide range of σ values the performance of the PGD attack increases. This is exemplified in Figure 2A for the MNIST dataset ($\epsilon = 0.3$).

Sampling: In an additional experiment we evaluated the number of sampling operations N that are the most effective for SNGD-based attacks. Each sampling operation N increases the computational overhead of SNGD-based attacks but should in turn improve the calculated descent direction. Therefore, we evaluated the success rate for different σ values and number of sampling operations on the MNIST validation set. Figure 2B illustrates that 4 sampling operations were optimal to increase the success rate for MNIST. We set $N = 4$ for all datasets for the remaining experiments.

Results and Discussion

Success Rate

Table 1 demonstrates that the proposed SN-PGD attack surpasses the mean success rate of prior attacks in our experiments. Nevertheless, for the TRADES model trained on the

CIFAR10 dataset the B&B attack was more effective than our approach. In contrast to the results reported in (Brendel et al. 2019) the B&B attack did not always outperform the standard PGD attack for the adversarially trained models. We could also not see a consistent increase in performance when combining SN-PGD or PGD and Nesterov momentum denoted by SN-N-PGD and N-PGD. N-PGD outperformed PGD in 3 out of 8 cases and SN-N-PGD outperformed SN-PGD in 1 out of 8 cases. We additionally analyzed the performance for individual runs as the standard deviation was high in some cases (e.g., F-MNIST). We observed that in general, the individual models were either more robust or vulnerable against all attacks. For all experiments where SN-PGD showed the highest mean success rate it also showed the highest success rate for all individual models. An exception was a single individual run (CIFAR10, PGD training), in which it was surpassed by the B&B attack.

Additional experiments

The following section summarizes additional experiments: 1) combination of SNGD with ODI, 2) combination of SNGD with noise decay, 3) different approaches to weight the gradients sampled with SNGD, 4) the runtime between different attacks, 5) the ability to approximate the global descent direction between GD- and SNGD-based attacks, and 6) the effectiveness of SNGD on increasingly convex loss surfaces.

1) Combination with ODI We evaluated if combining the different PGD-based attacks with Output Diversified Initialization (ODI) increases their success rate. From Table 2 we can see the accuracy and accuracy difference after combining the attacks with ODI. In 9 out of 24 cases the success rate improved while it decreased in 4 out of 24. For the PGD trained CIFAR10 model initialization with ODI improved the SN-PGD attack the most by 2.2%. For the remaining experiments the performance was not changed considerably. This is in line with the original paper, where the success rate increased only marginally on the MNIST dataset and more substantially on CIFAR10 (Tashiro, Song, and Ermon 2020). Note that ODI was partly designed to increase the transferability of adversarial attacks to other models which was not tested in this experiment.

2) Noise decay Madry et al. demonstrate that individual runs of a PGD attack converge to distinctive optima with similar loss values. Based on this observation, they concluded that that PGD might be an optimal first-order adversary. We noticed that SN-PGD converges to different loss values than PGD and further evaluated if different noise levels σ are optimal for different samples, as the characteristics of the loss surface are likely to change between different samples. Therefore, we evaluated if decaying the noise during a SN-PGD attack and between restarts improves the success rate. The idea is that decaying the noise during the attack should make the optimization more stable, as it is less likely that the algorithm alternates around a local optimum. A similar approach has also been proposed for the gradient sampling methodology (Burke, Lewis, and Overton 2005). We compared three different decay schedules: 1) decaying

	Clean	FGSM	PGD	N-PGD	B&B	SN-PGD	SN-N-PGD	SPSA
MNIST								
RFGSM	99.2 \pm 0	96.4 \pm 2	88.8 \pm 3	88.6 \pm 4	87.0 \pm 3	86.4 \pm 2	88.8 \pm 3	92.8 \pm 3
PGD	99.0 \pm 0	97.0 \pm 2	92.4 \pm 2	93.6 \pm 2	91.0 \pm 4	90.8 \pm 1	91.2 \pm 2	95.0 \pm 3
TRADES	99.5	96.2	91.2	91.6	90.6	90.4	91.3	92.2
F-MNIST								
RFGSM	85.4 \pm 1	74.8 \pm 4	60.4 \pm 8	61.6 \pm 8	60.6 \pm 9	58.8 \pm 8	61.0 \pm 9	66.6 \pm 8
PGD	85.7 \pm 0	83.2 \pm 5	70.0 \pm 7	69.2 \pm 7	70.8 \pm 7	68.8 \pm 6	68.6 \pm 6	74.2 \pm 6
CIFAR10								
RFGSM	83.6 \pm 0	54.0 \pm 7	43.4 \pm 6	44.0 \pm 4	45.8 \pm 5	43.0 \pm 6	44.6 \pm 5	49.1 \pm 6
PGD	79.7 \pm 0	55.0 \pm 3	48.4 \pm 2	49.6 \pm 2	49.0 \pm 3	48.2 \pm 2	49.2 \pm 3	50.5 \pm 4
TRADES	84.9	63.2	59.3	59.2	58.3	58.5	59.0	60.2

Table 1: Mean accuracy and standard deviation (%) on **MNIST**, **Fashion-MNIST** and **CIFAR10** for various adversarial attacks. The lower the accuracy the better (higher success rate). The attack with the highest success rate is displayed in bold for each row. RFGSM- and PGD-trained models were trained and evaluated five times.

ODI	PGD	N-PGD	SN-PGD
MNIST			
RFGSM	88.6 (-0.2)	88.4(-0.2)	86.8 (+0.4)
PGD	92.4(+0.0)	93.3(-0.3)	90.8 (+0.0)
TRADES	91.2 (+0.0)	91.4(-0.2)	90.3 (-0.1)
F-MNIST			
RFGSM	60.4(+0.0)	61.4(-0.2)	59.2 (+0.4)
PGD	70.0(+0.0)	69.2(+0.0)	68.8 (+0.0)
CIFAR10			
RFGSM	43.7(+0.3)	44.4(+0.4)	43.2 (+0.2)
PGD	48.4(+0.0)	49.6(+0.0)	46.0 (-2.2)
TRADES	57.5(-1.8)	57.7(-1.5)	56.8 (-1.7)

Table 2: Mean accuracy (%) on **MNIST**, **Fashion-MNIST** and **CIFAR10** for various adversarial attacks with ODI. The performance difference to attacks without ODI is given by a subscript (negative subscript values indicate an attack success rate increase). The attack with the highest success rate (With or without ODI) is displayed in bold for each row. RFGSM- and PGD-trained models were trained and evaluated five times.

	SN-PGD	+ID	+RD	+IRD
MNIST				
RFGSM	86.4 \pm 2	85.8 \pm 2	86.0 \pm 3	86.2 \pm 3
PGD	90.8 \pm 1	90.2 \pm 2	90.2 \pm 2	90.4 \pm 2
TRADES	90.4	90.0	90.4	90.1
F-MNIST				
RFGSM	58.8 \pm 8	58.0 \pm 9	58.4 \pm 9	57.8 \pm 9
PGD	68.8 \pm 6	67.4 \pm 6	68.0 \pm 6	67.6 \pm 6
CIFAR10				
RFGSM	43.0 \pm 6	42.8 \pm 3	43.0 \pm 5	43.0 \pm 5
PGD	48.2 \pm 2	48.2 \pm 2	48.0 \pm 1	47.8 \pm 2
TRADES	58.5	58.0	58.4	58.0

Table 3: Mean accuracy and standard deviation (%) on **MNIST**, **Fashion-MNIST** and **CIFAR10** for various SNGD-based adversarial attacks with different noise decay schedules. The lower the accuracy the better (higher success rate). The attack with the highest success rate is displayed in bold for each row. RFGSM- and PGD-trained models were trained and evaluated five times.

the noise in each attack iteration (SN-PGD + ID), 2) decaying the noise at every attack restart (SN-PGD + RD), 3) decaying the noise at every iteration and restart (SN-PGD + IRD). The results are summarized in Table 3. Every schedule improved the performance on average. Note that we did not tune the hyperparameters for noise decay and divided the noise by 1.05 at each iteration and by 2 at each restart.

3) Gradient weighting The dimensionality of the optimization problem is high compared to the amount of sampling operations N . This makes it less likely that the SNGD algorithm behaves like it would in the limit of N . Thus, we explored heuristics to improve the convergence rate of the algorithm. Instead of computing the final gradient direction as the weighted average of the gradients of all samples,

we weighted the gradients according to their relation to the gradient at the original data point. We tested three different measurements and their reciprocals as weights: 1) Cosine similarity, 2) Euclidean distance, 3) Scalar-product. In our experiment weighting with the cosine similarity was the most effective approach. This reduced the sensitivity of the method to the standard deviation σ without reducing the performance of the attack. However, we must know the individual gradients of each sample in order to weigh them. Thus, we cannot sum up the activation during the forward-passes and calculate only the average gradient, but rather have to do one backward-pass for each forward-pass. This introduces a considerable additional computational overhead. Overall, averaging the gradients was more effective in our experiments with respect to runtime and success rate.

PGD	SN-PGD	B&B	SPSA
100% $\pm 4.9\%$	75% $\pm 1\%$	455% $\pm 49\%$	2134% $\pm 367\%$

Table 4: Mean relative runtime of several attacks compared to standard PGD on all datasets (**MNIST**, **Fashion-MNIST** and **CIFAR10**) for various adversarial attacks.

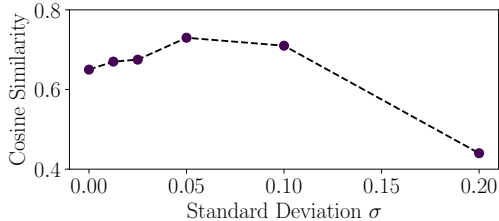


Figure 3: Average cosine similarity between subsequent gradients directions of a SN-PGD attack for varying standard deviations σ . For specific σ values the cosine-similarity between subsequent steps increases.

4) Runtime comparison Table 4 shows the runtime average and standard deviation for each attack over all experiments shown in Table 1. Due to the lack of gradient information, SPSA requires a high amount of model evaluations and takes by far the longest time to find adversarial examples. The B&B attack was also considerably slower than PGD for the same amount of model evaluations in our experiments. Note that in the beginning of each B&B attack, we need to find the decision boundary which introduces an additional computational overhead. The fastest attack was the proposed SN-PGD where we use the same amount of forward-passes as with the PGD attack but use less backward passes. We did not parallelize the sampling operations of SNGD in our experiments. The runtimes of the attacks were compared on a Nvidia Geforce GTX1080.

5) Approximation of the adversarial direction To get a better understanding of the effectiveness of SNGD, we inspected if SNGD-based PGD attacks approximate the final direction of a successful adversarial attack more accurately. This was achieved by computing the cosine similarity between subsequent iterations during the attack. Figure 3 shows that for the correct noise values σ the cosine similarity between subsequent attack iterations increases. Thus, the final adversarial direction is estimated more accurately by the SNGD-based attack. Depending on the characteristics of the loss surface the standard deviation σ of a SNGD-based attack can be adjusted to avoid improper local optima.

6) Loss surface After observing that SNGD can improve the approximation of the global descent direction we examined if SNGD has a bigger impact on models with non-convex loss surfaces, where the global descent direction is hard to approximate for standard GD. Therefore we calculated an approximate visualization of the loss landscape by calculating the loss value along the direction of a successful

adversarial perturbation (g) and a random orthogonal direction (g^\perp) originating from a clean sample as exemplified in Figure 4. In contrast to prior work (Kurakin et al. 2018; Chan et al. 2020) we found that the loss surface of the adversarial trained models (RFGSM and PGD) is often not increasing most rapidly towards the adversarial direction, which shows the non-convexity of the optimization problem. Furthermore, we noticed that in cases where the loss surface is less convex, the performance difference between PGD and SN-PGD increases. The sub-figures (A), (B), and (C) show loss surfaces which are increasingly convex, simultaneously the performance difference between SN-PGD and PGD for these models decreases ((A):4.1%, (B): 1.2%, (C): 0.1%). Table 1 shows that the difference between SN-PGD and PGD is higher for RFGSM-trained networks, where we generally observed that the loss surface is less convex. Note that this kind of loss surface visualization is limited and provides only an approximation of the true characteristics.

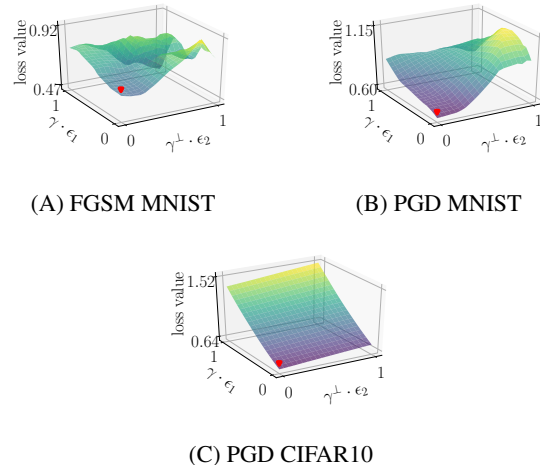


Figure 4: Representative loss surfaces around a clean sample X_i (red dot) for a fast FGSM-trained model (A) and PGD-trained models (B), (C). We calculate the loss value for sample $x_i + \epsilon_1 \cdot \gamma + \epsilon_2 \cdot \gamma^\perp$ where γ is the direction of a successful adversarial attack and γ^\perp a random orthogonal direction.

Conclusion

In this paper, we propose Sampled Nonlocal Gradient Descent (SNGD), an easy to implement modification of gradient descent to improve its convergence for non-convex and noisy loss surfaces. Through our experiments on three different datasets, we demonstrate that this method can be effectively combined with state-of-the-art adversarial attacks to achieve higher success rates. Furthermore, we show that SNGD-based attacks are more query efficient than current state-of-the-art attacks. Although the method proved to be effective in our experiments, larger datasets like ImageNet (Deng et al. 2009) still need to be explored. Additionally, the performance of the attack on alternative defense methods can be tested.

References

- Athalye, A.; Carlini, N.; and Wagner, D. A. 2018. Obfuscated Gradients Give a False Sense of Security: Circumventing Defenses to Adversarial Examples. In *Proceedings of the 35th International Conference on Machine Learning*, 274–283.
- Brendel, W.; Rauber, J.; Kümmeler, M.; Ustyuzhaninov, I.; and Bethge, M. 2019. Accurate, reliable and fast robustness evaluation. In *Advances in Neural Information Processing Systems 32*, 12861–12871.
- Burke, J. V.; Lewis, A. S.; and Overton, M. L. 2005. A Robust Gradient Sampling Algorithm for Nonsmooth, Non-convex Optimization. *SIAM J. Optim.* 15(3): 751–779. doi: 10.1137/030601296.
- Chan, A.; Tay, Y.; Ong, Y.; and Fu, J. 2020. Jacobian Adversarially Regularized Networks for Robustness. In *International Conference on Learning Representations, ICLR*.
- Deng, J.; Dong, W.; Socher, R.; Li, L.-J.; Li, K.; and Fei-Fei, L. 2009. Imagenet: A large-scale hierarchical image database. In *IEEE Conference on Computer Vision and Pattern Recognition, CVPR*, 248–255.
- Dong, Y.; Liao, F.; Pang, T.; Su, H.; Zhu, J.; Hu, X.; and Li, J. 2018. Boosting Adversarial Attacks With Momentum. In *IEEE/CVF Conference on Computer Vision and Pattern Recognition, CVPR*, 9185–9193.
- Du, Q. 2019. *Nonlocal Modeling, Analysis, and Computation: Nonlocal Modeling, Analysis, and Computation*. SIAM.
- Goodfellow, I.; Shlens, J.; and Szegedy, C. 2015. Explaining and harnessing adversarial examples. In *International Conference on Learning Representations, ICLR*.
- Guo, C.; Rana, M.; Cisse, M.; and van der Maaten, L. 2018. Countering Adversarial Images using Input Transformations. In *International Conference on Learning Representations, ICLR*. URL <https://openreview.net/forum?id=SyJ7CIWCb>.
- He, K.; Zhang, X.; Ren, S.; and Sun, J. 2016. Deep Residual Learning for Image Recognition. In *IEEE Conference on Computer Vision and Pattern Recognition, CVPR*, 770–778.
- Kingma, D. P.; and Ba, J. 2015. Adam: A Method for Stochastic Optimization. In *International Conference on Learning Representations, ICLR*. URL <http://arxiv.org/abs/1412.6980>.
- Krizhevsky, A. 2009. Learning multiple layers of features from tiny images. Technical report. doi:10.1.1.222.9220.
- Krizhevsky, A.; Sutskever, I.; and Hinton, G. E. 2012. ImageNet Classification with Deep Convolutional Neural Networks. In *Advances in Neural Information Processing Systems 25*, 1097–1105.
- Kurakin, A.; Boneh, D.; Tramèr, F.; Goodfellow, I.; Kurakin, A.; Brain, G.; Papernot, N.; Goodfellow, I.; Boneh, D.; and McDaniel, P. 2018. Ensemble adversarial training: Attacks and defenses. In *International Conference on Learning Representations, ICLR*. URL <https://openreview.net/forum?id=rkZvSe-RZ>.
- Kurakin, A.; Goodfellow, I. J.; and Bengio, S. 2017. Adversarial examples in the physical world. In *International Conference on Learning Representations, ICLR, Workshop Track Proceedings*. URL <https://openreview.net/forum?id=HJGU3Rodl>.
- LeCun, Y.; Bottou, L.; Bengio, Y.; Haffner, P.; et al. 1998. Gradient-based learning applied to document recognition. *Proceedings of the IEEE* 86(11): 2278–2324.
- Lin, J.; Song, C.; He, K.; Wang, L.; and Hopcroft, J. E. 2020. Nesterov Accelerated Gradient and Scale Invariance for Adversarial Attacks. In *International Conference on Learning Representations*. URL <https://openreview.net/forum?id=SJIHwkBYDH>.
- Madry, A.; Makelov, A.; Schmidt, L.; Tsipras, D.; and Vladu, A. 2018. Towards Deep Learning Models Resistant to Adversarial Attacks. In *International Conference on Learning Representations*. URL <https://openreview.net/forum?id=rJzIBfZAb>.
- Samangouei, P.; Kabkab, M.; and Chellappa, R. 2018. Defense-GAN: Protecting Classifiers Against Adversarial Attacks Using Generative Models. In *International Conference on Learning Representations*. URL <https://openreview.net/forum?id=BkJ3ibb0->.
- Smith, L. N. 2017. Cyclical Learning Rates for Training Neural Networks. In *IEEE Winter Conference on Applications of Computer Vision*, 464–472.
- Spall, J. C. 1992. Multivariate stochastic approximation using a simultaneous perturbation gradient approximation. *IEEE Transactions on Automatic Control* 37(3): 332–341.
- Szegedy, C.; Zaremba, W.; Sutskever, I.; Bruna, J.; Erhan, D.; Goodfellow, I. J.; and Fergus, R. 2014. Intriguing properties of neural networks. In *International Conference on Learning Representations, ICLR*. URL https://openreview.net/forum?id=kklr_MTHMRQjG.
- Tashiro, Y.; Song, Y.; and Ermon, S. 2020. Diversity can be Transferred: Output Diversification for White- and Black-box Attacks. <https://arxiv.org/abs/2003.06878>.
- Tramèr, F.; and Boneh, D. 2019. Adversarial Training and Robustness for Multiple Perturbations. In *Advances in Neural Information Processing Systems 32*, 5866–5876.
- Uesato, J.; O’Donoghue, B.; Kohli, P.; and van den Oord, A. 2018. Adversarial Risk and the Dangers of Evaluating Against Weak Attacks. In *Proceedings of the 35th International Conference on Machine Learning, ICML*, 5025–5034.
- van den Oord, A.; Dieleman, S.; Zen, H.; Simonyan, K.; Vinyals, O.; Graves, A.; Kalchbrenner, N.; Senior, A. W.; and Kavukcuoglu, K. 2016. WaveNet: A Generative Model for Raw Audio. In *The 9th ISCA Speech Synthesis Workshop*, 125.
- Wong, E.; Rice, L.; and Kolter, J. Z. 2020. Fast is better than free: Revisiting adversarial training. In *International Conference on Learning Representations*. URL <https://openreview.net/forum?id=BJx040EFvH>.
- Xiao, H.; Rasul, K.; and Vollgraf, R. 2017. Fashion-MNIST: a Novel Image Dataset for Benchmarking Machine

Learning Algorithms. <https://github.com/zalandoresearch/fashion-mnist>.

Zhang, H.; Yu, Y.; Jiao, J.; Xing, E. P.; Ghaoui, L. E.; and Jordan, M. I. 2019. Theoretically Principled Trade-off between Robustness and Accuracy. In *Proceedings of the 36th International Conference on Machine Learning, ICML, Long Beach, California, USA, 7472–7482*.